Conformational Studies of the Tetramerization Site of Human Erythroid Spectrin by Cysteine-Scanning Spin-Labeling EPR Methods†

Shahila Mehboob,‡,§,|| Bing-Hao Luo,‡,||,# Wentao Fu,§ Michael E. Johnson,§ and L. W.-M. Fung*,^,||

Department of Chemistry, University of Illinois at Chicago, 845 West Taylor Street, Chicago, Illinois 60607, Center of Pharmaceutical Biotechnology, University of Illinois at Chicago, 900 South Ashland Avenue, Chicago, Illinois 60607, and Department of Chemistry, Loyola University of Chicago, 6525 North Sheridan Road, Chicago, Illinois 60626

Received May 27, 2005; Revised Manuscript Received August 9, 2005

ABSTRACT: We used cysteine-scanning and spin-labeling methods to prepare singly spin labeled recombinant peptides for electron paramagnetic resonance studies of the partial domain regions at the tetramerization site (N-terminal end of α and C-terminal end of β) of erythroid spectrin. The values of the inverse line width parameter (ΔH_0^{-1}) from a family of SpαI-1−368Δ peptides scanning residues 21−30 exhibited a periodicity of ∼3.5−4. We used molecular dynamics calculations to show that the asymmetric mobility of this helix is not necessarily due to tertiary contacts, but is likely due to intrinsic properties of helix C′, a helix with a heptad pattern sequence. The residues with low ΔH_0^{-1} values (residues at positions 21, 25, and 28/29) were those on the hydrophobic side of this amphipathic helix. Native gel electrophoresis results showed that these residues were functionally important and are involved in the tetramerization process. Thus, EPR results readily identified functionally important residues in the α spectrin partial domain region. Mutations at these positions may lead to clinical symptoms. Similarly, the ΔH_0^{-1} values from a family of spin-labeled SpβI-1898−2083Δ peptides also exhibited a periodicity of ∼3.5−4, indicating a helical conformation in the two scanned regions (residues 2008−2018 and residues 2060−2070). However, the region consisting of residues 2071−2076 was in a disordered conformation. Both helical regions include a hydrophilic side with high ΔH_0^{-1} values and a hydrophobic side with low ΔH_0^{-1} values, demonstrating the amphipathic nature of the helical regions. Residues 2008, 2011, 2014, and 2018 in the first scanned region and residues 2061, 2065, and 2068 in the second scanned region were on the hydrophobic side. These residues were critical in αβ spectrin association at the tetramerization site. Mutations at some of these positions have been reported to be detrimental in clinical studies.

Spectrin, a member of the spectrin superfamily and a major protein in the membrane (cyto)skeleton, is ubiquitous among vertebrate tissues, as well as in simple metazoans, implying that spectrin plays a fundamental role in cells (*1*−*9*). After first being identified in erythrocytes (*10*), many distinct spectrin isoforms have since been discovered.

Several functions of spectrin involve its interactions with other components [spectrin−actin interaction, spectrin−membrane interaction, spectrin−ion channel interaction, etc. (*3*)], yet some of the most fundamental functions of spectrin involve spectrin "self-association" {two heterodimers (αβ) associating to form a functional tetramer [(αβ)$_2$] (*11*)}. Several hereditary hemolytic anemia diseases involve single-amino acid mutations in spectrin that destabilize its tetramers, resulting in low levels of spectrin tetramers and high levels of dimers (*4*, *12*, *13*). Thus, the tetramerization site is an important functional site for most spectrin isoforms. The best studied spectrin tetramer is that from human erythrocyte [(αIβI)$_2$].

The tetramerization site consists of the N-terminal region of the α subunit (αN)[1] and the C-terminal region of the β subunit (βC). Tetramer formation involves a pair of αN−βC (α_1N−β_2C and α_2N−β_1C) associations to give an $\alpha_1\beta_2\alpha_2\beta_1$ tetramer (*14*−*17*). At the other end of the spectrin molecule, the C-terminal region of the α subunit and the N-terminal region of the β subunit associate with higher affinity, and these regions are termed the nucleation site. We assume that these two major assembly sites (the dimerization/nucleation site and the tetramerization site) are *independent*

† This work was supported by grants from the American Heart Association Midwest Affiliate (Grant-in-Aid to L.W.-M.F., predoctoral fellowships to S.M. and B.-H.L.) and NIH (to L.W.-M.F. and M.E.J.).

* To whom correspondence should be addressed: University of Illinois at Chicago, 845 W. Taylor St., MC 111, Chicago, IL 60607-7061. Telephone: (312) 355-5516. Fax: (312) 996-0431.

‡ These authors contributed equally to this work.

§ Center of Pharmaceutical Biotechnology, University of Illinois at Chicago.

Current address: The CBR Institute for Biomedical Research and Department of Pathology, Harvard Medical School, 200 Longwood Ave., Boston, MA 02115.

^ Department of Chemistry, University of Illinois at Chicago.

|| Loyola University of Chicago.

[2] Abbreviations: αN, N-terminal region of the α subunit; βC, C-terminal region of the β subunit; CD, circular dichroism; DTT, dithiothreitol; EPR, electron paramagnetic resonance; ΔH_0^{-1}, inverse line width parameter; helix C′, α partial domain; M_s, scaled mobility parameter; MTSSL, (1-oxy-2,2,5,5-tetramethyl-3-pyrrolinyl-3-methyl)-methanethiosulfonate spin-label; PBS, 5 mM phosphate buffer (pH 7.4) containing 150 mM NaCl; SpαI, erythroid α spectrin; SpβI, erythroid β spectrin; TFE, 2,2,2-trifluoroethanol.

10.1021/bi051009m CCC: $30.25
Published on Web 11/04/2005

sites (*18*, *19*). On the basis of this premise, we use recombinant peptides of spectrin fragments as model systems for specific regions of spectrin to study the local structures at the tetramerization site of spectrin.

On the basis of sequence homology, it has long been suggested that both αN and βC regions of erythroid spectrin consist of partial domains, with a single helix for the αN region and two helices for the βC region (*15*, *20*). Currently, only the structure of the N-terminal region of erythroid α spectrin (SpαI) has been determined experimentally by NMR methods. The solution NMR structures of a recombinant peptide that consists of the first 156 residues of SpαI show that the first 20 residues preceding and the seven residues following the first helix (helix C′) are in a disordered conformation (*21*). The three subsequent helices (helices A_1−C_1) form a triple-helical bundle structural domain that is similar, but not identical, to previously published structures for spectrin from *Drosophila* (*22*) and chicken brain (*23*). However, no experimental structural information is available for β spectrin at the tetramerization site.

In this study, we use cysteine-scanning and spin-labeling methods to prepare singly labeled recombinant, erythroid α and β spectrin peptides for electron paramagnetic resonance (EPR) studies. Site-directed cysteine-scanning spin-label EPR studies have become a powerful tool for monitoring the structure and dynamics of protein systems that are not easily studied by either NMR or X-ray methods (*24*, *25*).

MATERIALS AND METHODS

Spectrin Recombinant Peptides. The SpαI-1−368, SpαI-1−156, and SpβI-1898−2083 peptides were prepared as described previously (*19*, *26*). SpαI-1−368 is a peptide with the first 368 amino acid residues of SpαI, consisting of the partial domain and the first three structural domains; SpαI-1−156 is a peptide with the first 156 amino acid residues, consisting of the partial domain and the first structural domain (*27*). SpβI-1898−2083 is a peptide with the sequence of amino acid residues 1898−2083, a region being considered to consist of the last structural domain followed by the partial domain in SpβI (*19*). A cysteine-less peptide derived from SpβI-1898−2083 with cysteine residues at positions 1962 and 2012 replaced with alanine residues (SpβI-1898−2083-cysteine-less) was prepared first. With this peptide, 11 single-cysteine peptides scanning positions 2008−2018 (βL2008C, βL2009C, βE2010C, βV2011C, βC2012, βQ2013C, βF2014C, βS2015C, βR2016C, βD2017C, and βA2018C) and 17 single-cysteine peptides scanning positions 2060−2076 (βS2060C, βW2061C, βA2062C, βE2063C, βR2064C, βF2065C, βA2066C, βA2067C, βL2068C, βE2069C, βK2070C, βP2071C, βT2072C, βT2073C, βL2074C, βE2075C, and βL2076C) were then prepared, using the pGEX-2T vector containing the cDNA for SpβI-1898−2083-cysteine-less as the template, and primers designed to introduce a cysteine at a specific position for each peptide. On the basis of the sequence homology alignment, we have proposed a working model for the structure of the two helices (helix A′ and helix B′) in the SpβI partial domain (*19*). In this working model, helix A′ begins at residue 2008 and ends at residue 2037 while helix B′ begins at residue 2044 and ends at residue 2072. We have also shown that recombinant peptides that terminate at positions 2072 and 2073 associate with an α peptide, whereas the peptides that terminate at a position prior to residue 2072 do not associate with the α peptide (*27*). Thus, we scanned the region that presumably consists of the beginning of helix A′ (residues 2008−2018) and a region that consists of the end of helix B′ (residues 2060−2076). These 28 peptides were collectively termed βΔ peptides.

Each DNA fragment inserted into the pGEX-2T vector was sequenced, and only those that were confirmed to have incorporated the cysteine residue as well as the positions of the start and stop codons were used for protein expression.

Similarly, a SpαI-1−368-cysteine-less peptide with the three native cysteine residues sequentially replaced with alanine residues (*27*) and 10 single-cysteine peptides scanning positions 21−30 in SpαI-1−368 (αA21C, αE22C, αE23C, αI24C, αQ25C, αE26C, αR27C, αR28C, αQ29C, and αE30C) were prepared. These peptides were collectively termed as αΔ peptides.

All peptides were purified by thrombin cleavage from the GST fusion protein following standard laboratory methods (*28*). As part of the thrombin recognition sequence, residues G and S remained as the first two residues in all peptides after thrombin cleavage. Peptide identity and purity were checked by polyacrylamide gel electrophoresis and mass spectrometry using electrospray ionization techniques. Protein concentrations were determined with absorbance values at 280 nm, using extinction coefficient values determined from the primary sequence (31 010 cm^{-1} M^{-1} for all peptides in the SpβI-1898−2083 family except for βW2061C, for which a value of 25 320 cm^{-1} M^{-1} was used; 16 500 cm^{-1} M^{-1} for SpαI-1−156; and 50 070 cm^{-1} M^{-1} for peptides in the SpαI-1−368 family). Each peptide was analyzed by circular dichroism (CD) methods (*19*) to ensure its folding integrity.

Native Gel Electrophoresis. The association of spin-labeled peptides of the SpβI-1898−2083 family with SpαI-1−156 and of the SpαI-1−368 family with SpβI-1898−2083 were monitored by native gel electrophoresis (*19*). The α (10 μM) and β (20 μM) peptides were added in a 1:2 molar ratio (total of 4 μg) and incubated in 5 mM phosphate buffer (pH 7.4) containing 150 mM NaCl (PBS7.4) at 4 °C for ∼16 h before electrophoresis was carried out with a 6% native polyacrylamide gel (*19*).

Spin Labeling. The single-cysteine α or β peptides were mixed with dithiothreitol (DTT) at 37 °C for 1 h to reduce the cysteine residue, followed by size-exclusion column chromatography to remove DTT and incubation with a 5-fold molar excess of spin label (1-oxy-2,2,5,5-tetramethyl-3-pyrrolinyl-3-methyl)methanethiosulfonate (MTSSL) (Toronto Research Chemicals, Toronto, ON) for 3 h at room temperature in the dark. To determine background labeling, cysteine-less samples (SpβI-1898−2083Δ and SpαI-1−368Δ) were also processed, in parallel. Excess spin-labels were removed with size-exclusion column chromatography. The concentrations of spin-labels bound to each peptide were determined from spectra of labeled samples without sucrose additions. The peptide concentrations were determined from the absorbance values at 280 nm, as indicated above. The concentration ratio of the spin-label to the peptide was calculated for each peptide. Generally, ∼10−15% background labeling was observed in cysteine-less samples, and thus, this was subtracted to give the number of spin-labels per protein molecule.

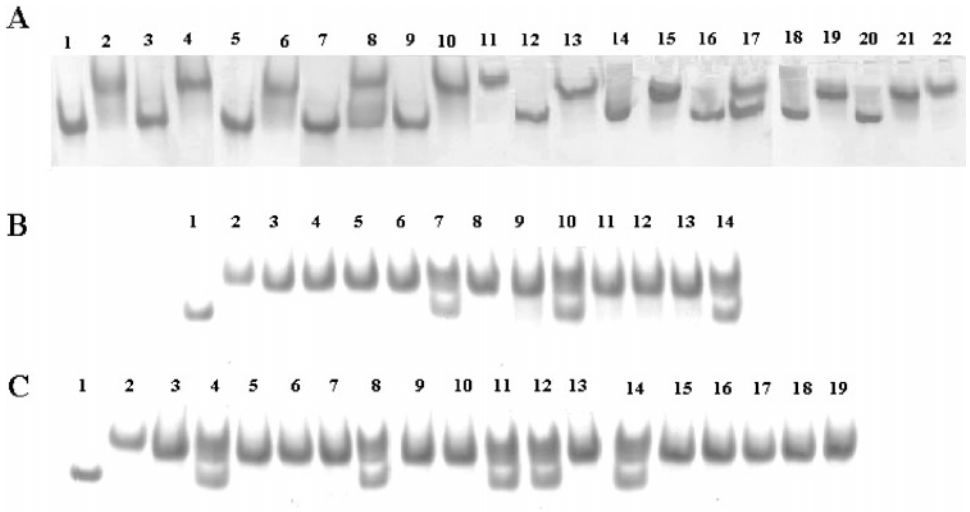

FIGURE 1: Native polyacrylamide gel (6%) electrophoresis to determine the association of spin-labeled α peptides with Spβ I-1898−2083 (A) and spin-labeled β peptides with SpαI-1−156 (B and C). Each sample contained ∼4 μg of protein. The gels were run at 20 °C in 40 mM Tris, 20 mM sodium acetate, and 2 mM EDTA at pH 7.4. (A) For lanes 1−10, the odd-numbered lanes were loaded with the following α peptides sequentially: αA21C (lane 1), αE22C (lane 3), αE23C (lane 5), αI24C (lane 7), and αQ25C (lane 9). The R_f values of the band in these lanes were ∼0.51. The even-numbered lanes were loaded with corresponding α peptides (10 μM) with Spβ I-1898−2083 (20 μM). For example, αA21C and Spβ I-1898−2083 were in lane 2. The appearance of a band with R_f values of ∼0.31, the R_f value for Spβ I-1898−2083, and the disappearance of the band with R_f values of ∼0.51 in these even-numbered lanes demonstrated the association of the limiting α peptide with excess Spβ I-1898−2083. Thus, the results show that αA21C (lane 2), αE22C (lane 4), αE23C (lane 6), and αQ25C (lane 10) associated with Spβ I-1898−2083, but αI24C (lane 8) did not. The Spβ I-1898−2083 sample was loaded into lanes 11 and 22. For lanes 12−21, even-numbered lanes were loaded with α peptides: αE26C (lane 12), αR27C (lane 14), αR28C (lane 16), αQ29C (lane 18), and αE30C (lane 20). The odd-numbered lanes were loaded with corresponding α peptides with Spβ I-1898−2083. For example, αE26C and Spβ I-1898−2083 were in lane 13. The results show that peptides αE26C (lane 13), αR27C (lane 15), αQ29C (lane 19), and αE30C (lane 21) associated with Spβ I-1898−2083, but αR28C (lane 17) did not. (B) Association of SpαI-1−156 with single-cysteine β peptides scanning residues 2008−2018. Lane 1 was loaded with SpαI-1−156, lane 2 with cysteine-less Spβ I-1898−2083, and lane 3 with their mixtures. Lanes 4−14 were mixtures of SpαI-1−156 (10 μM) with an individual single cysteine β peptide (20 μM): βL2008C (lane 4), βL2009C (lane 5), βE2010C (lane 6), βV2011C (lane 7), βC2012 (lane 8), βQ2013C (lane 9), βF2014C (lane 10), βS2015C (lane 11), βR2016C (lane 12), βD2017C (lane 13), and βA2018C (lane 14). These data suggest that all β peptides associated with SpαI-1−156 except βV2011C, βF2014C, and βA2018C. (C) Association of SpαI-1−156 with single-cysteine β peptides scanning residues 2060−2076. Lane 1 was loaded with SpαI-1−156 and lane 2 with cysteine-less Spβ I-1898−2083. Lanes 3−19 were mixtures of SpαI-1−156 (10 μM) with individual β peptides (20 μM): βS2060C (lane 3), βW2061C (lane 4), βA2062C (lane 5), βE2063C (lane 6), βR2064C (lane 7), βF2065C (lane 8), βA2066C (lane 9), βA2067C (lane 10), βL2068C (lane 11), βE2069C (lane 12), β K2070C (lane 13), βP2071C (lane 14), βT2072C (lane 15), βT2073C (lane 16), βL2074C (lane 17), βE2075C (lane 18), and βL2076C (lane 19). These results show that all β peptides, except βW2061C, βF2065C, βL2068C, βE2069C, and βP2071C, associated with SpαI-1−156.

EPR Studies. The spin-labeled EPR samples (∼100 μM) were in PBS7.4 in the presence or absence of 30% sucrose. The addition of sucrose reduces the contribution of the overall motion of the protein to the EPR spectral line shape (*29*). Some samples of α peptides also included 60% 2,2,2-trifluoroethanol (TFE). Spectra were acquired at 21 °C with a Varian E109 spectrometer equipped with a TM 102 cavity at 9.41 GHz (X-band). After the removal of background signals (see Spin Labeling), the spectra were normalized to represent the same number of spins, as determined by the double-integration method. The inverse values of the peak-to-peak line width of the central resonance signal (ΔH^{-1}) were obtained from EPR spectra of samples in 30% sucrose. Each ΔH^{-1} value was scaled according to the maximum and minimum ΔH^{-1} values in the family of peptides to give a scaled mobility parameter M_s, a parameter that reflects changes in both the ordering and mobility of the nitroxide motion and was easier to measure even in spectra with poor signal-to-noise ratios (*25*), as in β peptides which exhibited lower solubilities than α peptides.

Molecular Dynamics Calculations. The NMR structure for the region consisting of residues 21−45 (helix C′) was used as the starting structure for energy minimization until the root-mean-square deviation (rmsd) was less than 0.1 kcal mol^{-1} Å^{-1}. The resulting single helix was then surrounded with water molecules (a total of 3714), which extended 10 Å from the helix surface, in a periodic box (51.7 Å × 58.1 Å × 50.3 Å) with a TIP3P potential (*30*). The energy minimization and molecular dynamics (MD) simulations were carried out with the SANDER module in AMBER7.0 (*31*) using the PARM99 force field (*32*). The particle mesh Ewald (PME) method (*33*) was then used for electrostatics, and SHAKE (*34*) was used for restricting motion of all covalent bonds involving hydrogen. MD simulations were carried out at 300 K and 1 atm with a time step of 2.0 fs and the nonbonded cutoff at 12.0 Å. The temperature during MD simulation was maintained by the Berendsen coupling algorithm (*35*). The total MD simulation time was 1000 ps. After equilibration for 200 ps, a total of 80 snapshots were collected every 10 ps for root-mean-square deviation calculations. The CARNAL module in AMBER7.0 (*31*) was used for rmsd calculation. First, an average structure was constructed by averaging the coordinates of the 80 snapshots. Then, each snapshot was overlapped with the average structure to calculate the rmsd value of each side chain.

RESULTS

Peptide Analysis. Densitometric analysis of SDS−PAGE gels indicated that all α and β peptides were at least 95% pure. Molecular masses from electrospray ionization mass

spectrometry were within 0.1% of the theoretical values. CD analysis of spin-labeled α and β peptides showed helicity contents similar to those of parent peptides (*19*), ranging from 60 to 70%, with α peptides ~10% higher than those for β peptides. βP2071C exhibited a slightly lower helical content (~45%). Spin labeling did not change the helicity values of the peptides. Addition of 30% sucrose to samples caused slight increases in their helicity values.

The spin-label to peptide molar ratio was found to be between 0.5 and 1.0 for all α and β peptides, with most around 1.

Association of Spin-Labeled α Peptides with the C-Terminal Region of β Spectrin. The association of SpαI-1−368 with Spβ I-1898−2083 in the micromolar concentration range (1:2 molar ratio of α and β) was easily visualized on a native gel due to the disappearance of the band corresponding to SpαI-1−368 ($R_f = 0.51$) and the appearance of a band corresponding to Spβ I-1898−2083 and the αβ complex ($R_f = 0.31-0.32$) (*19*). All α peptides (Figure 1A, lanes 2, 4, 6, 10, 13, 15, 19, and 21), except αI24C (lane 8) and αR28C (lane 17), were found to associate with Spβ I-1898−2083.

Association of Spin-Labeled β Peptides with the N-Terminal Region of α Spectrin. The SpαI-1−156 peptide, which is smaller than SpαI-1−368 but has an R_f value similar to that of SpαI-1−368 (*19*), was used as a model peptide to determine if the β peptides associated with the N-terminal region of α spectrin. Among the 28 single-cysteine β peptides, 20 β peptides (Figure 1B, lanes 4−6, 8, 9, and 11−13, and Figure 1C, lanes 3, 5−7, 9, 10, 13, and 15−19) associate with SpαI-1−156 in the micromolar concentration range. The eight remaining peptides [βV2011C (Figure 1B, lane 7), βF2014C (Figure 1B, lane 10), βA2018C (Figure 1B, lane 14), βW2061C (Figure 1C, lane 4), βF2065C (Figure 1C, lane 8), βL2068C (Figure 1C, lane 11), βE2069C (Figure 1C, lane 12), and βP2071C (Figure 1C, lane 14)] did not associate with SpαI-1−156 at micromolar concentrations.

EPR Measurements of the α Peptides. EPR spectra of the 10 spin-labeled α peptides, scanning positions 21−30, in PBS7.4 buffer show line shape variations in these spectra, and the variations became systematic for spectra of samples with 30% sucrose (Figure 2). For the spectra of samples in sucrose, the first and fifth positions exhibited very similar line shapes. For example, spectra with spin-labels at positions 21 (αA21C), 25 (αQ25C), and 29 (αQ29C) show distinctive multicomponent features with highly anisotropic motions for the nitroxide moiety, whereas those at positions 22 (αE22C), 26 (αE26C), and 30 (αE30C) reflect more mobile motions, similar to those of nitroxide labels with unrestricted motions on helix surfaces (*29*). Spectra with spin-labels at positions 23 (αE23C) and 27 (αR27C) are similar, representing nitroxide labels with greater flexibility, whereas those at positions 24 (αI24C) and 28 (αR28C) show more restricted motions.

A more quantitative examination of the ΔH_0^{-1} values in this series (Figure 3A) indicates that the maximum value was 0.38 (residues 22 and 26), and the minimum value was 0.25 (residue 28). Under similar sample and experimental conditions, values of ΔH_0^{-1} below 0.32 are often used to indicate relatively restricted motion, while values of ΔH_0^{-1} between 0.32 and 0.38 are indicative of less restricted motions such as those for residues on helix surfaces (*29*, *36*). The ΔH_0^{-1} values show a periodicity of 3.5−4 as a function of the residue position, suggesting a helical conformation in this region.

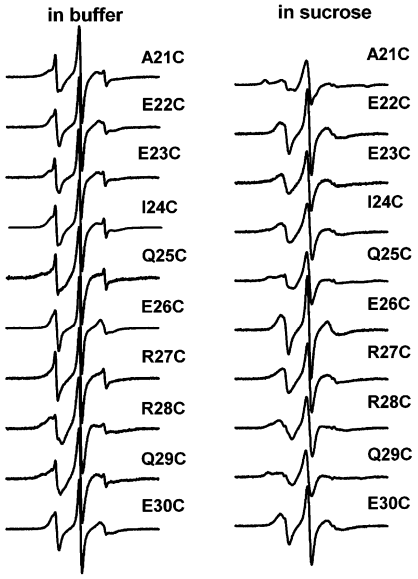

FIGURE 2: EPR spectra of spin-labeled α peptides scanning residues 21−30 in PBS7.4 buffer without (left column) and with 30% sucrose (right column) at 20 °C. The spectra were normalized to represent the same number of spins in each spectrum, as determined by double integration. The contribution of the background spin-label (see Materials and Methods) was subtracted from each spectrum.

For samples in 60% TFE [TFE is a solvent known to affect hydrogen bonding and solvent structure (see refs *37* and *38*) and thus hydrophobicity], the range of line shape variation became smaller, noticeably around positions 27−30 (Figure 3A). There also appeared to be a phase shift in the periodic pattern. The ΔH_0^{-1} values were shifted to higher values in 60% TFE than in 30% sucrose since the viscosity values of the samples in 60% TFE were much lower than those in 30% sucrose. The viscosity of TFE (100%) is ~1.78 cP (*38*, *39*), whereas the viscosity of 30% sucrose is ~3.19 cP (*40*).

The rmsd Values of the α Partial Domain Side Chains. The rmsd values from molecular dynamics calculations show various side chain flexibilities (Figure 3B). The values ranged from 0.29 to 0.84 Å, with residues 24 and 28 being less flexible and residues 22, 26, and 29 being more flexible. The average rmsd value of these 10 side chains was 0.60 Å. The rmsd variations (or side chain flexibilities) also exhibit a periodic pattern (Figure 3B), similar to that observed in EPR data (either ΔH_0^{-1}, Figure 3A, or M_s, Figure 3B, values). Thus, it appears that, even without tertiary contacts, the side chains on the hydrophobic side of the lone helix C′ are less flexible than those on the hydrophilic side of the helix.

EPR Studies of the β Peptides. The EPR spectra of the β peptides with spin-labels at positions 2008−2018 and 2060−2076 again exhibited a similar periodic pattern in either ΔH_0^{-1} (Figure 5A,C) or M_s (Figure 5B,D) values as a function of residue position. Spectra of the peptide with a spin-label at position 2008 exhibited highly anisotropic motion. Spectra at positions 2009−2018 as well as 2060−2070 were similar to those of α peptides scanning the beginning of helix C′ and similar to typical two-component

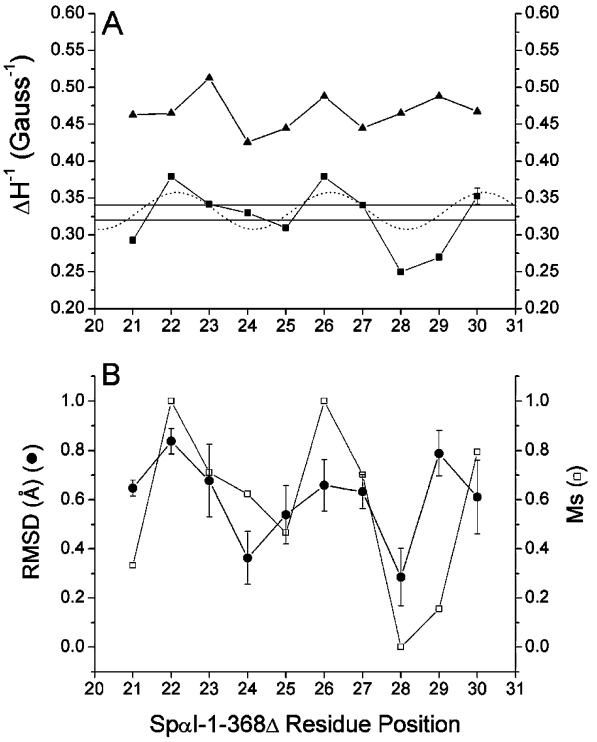

FIGURE 3: (A) Plot of the values of the inverse of the EPR central line width (ΔH^{-1}) vs residue number of α (SpαI-1−368) peptides in 30% sucrose (■) to show the periodic variation of ΔH^{-1} as a function of residue position. The dotted line is a sine wave with a periodicity of 4. Values of ΔH^{-1} of <0.32 are indicative of relatively restricted motion, whereas values of ΔH^{-1} of >0.34 are indicative of more mobile motions. A typical standard deviation error bar ($n = 3$) is shown at position 30. Also shown are the values of samples in the presence of 60% TFE (▲). (B) rmsd values (●) of residues 21−30 of αI spectrin obtained from energy minimization and molecular dynamics calculations in the presence of water molecules. The starting structure was obtained from NMR studies. The values of the scaled mobility parameter M_s (□), obtained from ΔH^{-1} values, followed similar periodic variations as a function of residue position.

spectra of spin-labeled side chains attached to a helical backbone (*29*). The $\Delta H_0^{-1}/M_s$ values (Figure 5) indicated that the flexibility of sequential residues oscillated between being more flexible to less flexible for spin-labels at positions 2008−2018 as well as positions 2060−2070. The periodicity of ∼3.5−4 corresponds with the periodicity of a helix. However, this periodicity pattern was not found for residues 2071−2076. The EPR spectra of these six positions were similar to those of a spin-labeled side chain with high flexibility, such as those in a loop or disordered conformation (*29*).

DISCUSSION

It has long been suggested that both α and β subunits of erythroid spectrin consist mostly of triple-helical bundle structural domains, and each with a partial domain at the tetramerization site (*20*). However, since these subunits are fairly large (consisting of more than 2000 amino acid residues) and flexible, detailed experimental information about the structure of intact spectrin is still not available. We, as well as many others, have used recombinant peptides to model functionally important segments of spectrin and determined structural and functional properties of these spectrin peptides (*19*, *21*, *26*, *27*).

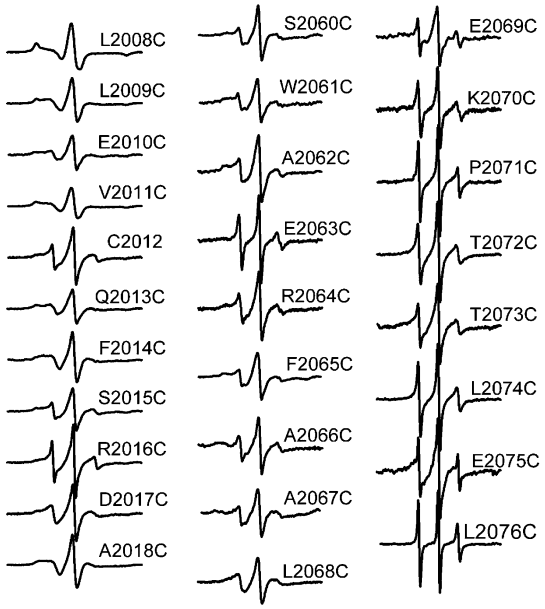

FIGURE 4: EPR spectra of spin-labeled β (SpβI-1898−2083) peptides scanning residues 2008−2018 and 2060−2076 in PBS7.4 buffer containing 30% sucrose at 20 °C. The spectra were normalized to represent the same number of spins in each spectrum, as determined by double integration. The contribution of the background spin-label was subtracted from each spectrum.

Structure of the α *Spectrin Partial Domain.* Our NMR studies of SpαI-1−156 showed that the α spectrin partial domain consists of a single helix (helix C′) and set the boundary of this helix as being from residue 21 to 45 (*21*). The first 20 residues in α spectrin exhibit a disordered conformation. Following residue 45 is a seven-residue (residues 46−52) disordered junction region. The first helix (helix A_1) of the first structural domain (residues 52−156) starts at position 53.

The sequence of helix C′ (residues 21−45), as well as the sequences of other helical regions in the structural domain, exhibits a seven-residue (heptad) periodicity. The predicted structure of a helix with a heptad pattern is a curved (coiled) helix, with the larger curvature side as the hydrophilic face and the smaller curvature side as the hydrophobic face of the helix (*41*, *42*), as seen in the coiled coils of the triple-helical domain region (*21*, *22*). However, because of resolution/sensitivity limitations in high-resolution NMR studies, the observed structures of helix C′ are presented as a symmetric (straight) helix, with no distinction between the hydrophilic and hydrophobic faces of the helix detected (*21*).

The cysteine-scanning spin-label EPR studies of the region consisting of residues 21−30 of SpαI-1−368 showed that the ΔH_0^{-1} values of the scanned residues exhibited a periodicity of 3.5−4, consistent with the helical nature predicted from sequence and observed by NMR measurements. The ΔH_0^{-1} values readily show the asymmetric nature of the helix. This side chain asymmetry in flexibility could potentially arise either from the hydrophobic moment of the helix (*43*, *44*) or due to the side chains in one side of the helix having tertiary contacts with other parts of the molecule.

Since the junction region (residues 46−52) is flexible, helix C′ may assume many orientations with respect to the triple-helical structural domain. It is physically possible to have many structures, from a structure with a lone helix extending out from the triple-helical bundle to a structure

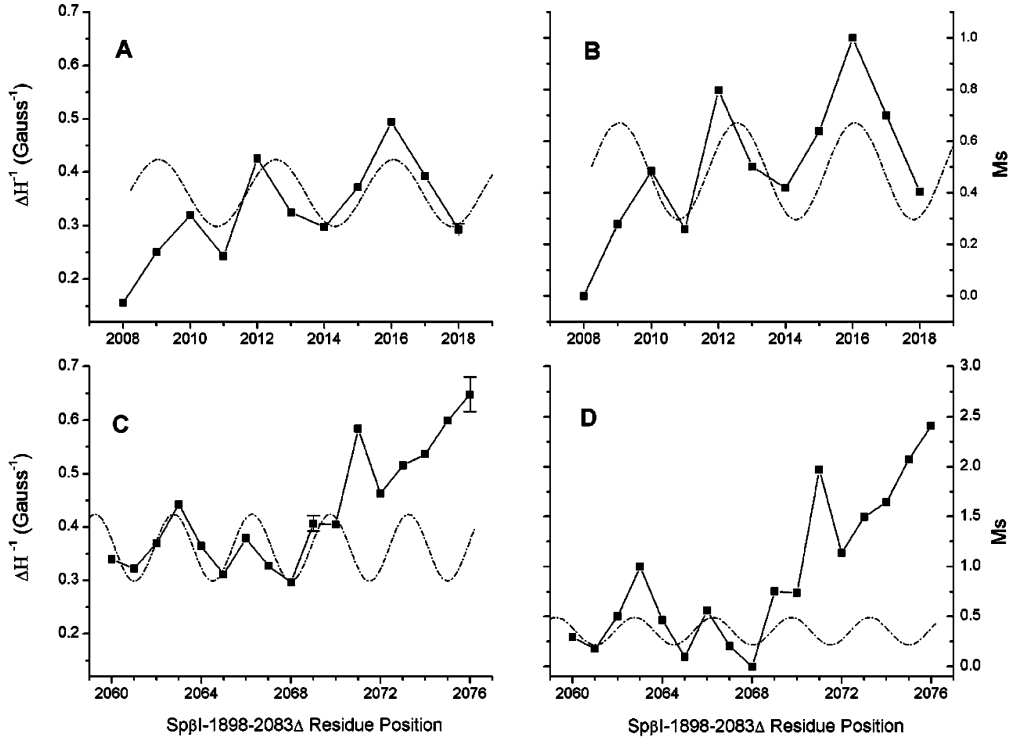

FIGURE 5: Plot of the values of ΔH^{-1} and M_s vs residue number of β (SpβI-1898−2083) peptides scanning residues 2008−2018 (A and B) and residues 2060−2076 (C and D) in PBS7.4 containing 30% sucrose, showing a periodic variation of $\Delta H^{-1}/M_s$ values as a function of residue position. The dotted lines are sine waves with a periodicity of 3.5. Typical standard deviation error bars of ΔH^{-1} are shown at positions 2018, 2069, and 2076 ($n = 3$).

with a four-helix bundle, and variations between them (*21*). We replaced residue 154 with cysteine, labeled with a spin-label, and found that several NMR resonances from the N-terminal region of helix C′ retained their intensities and were not broadened by the paramagnetic center of the spin-label. These NMR results unambiguously show that helix C′ does not bundle with the structural domain to form a four-helix bundle, and is a lone helix on the NMR time scale (milliseconds to seconds). Our CD data also show that helix C′ is a lone helix (*19*).

The MD calculations show that, in the presence of water molecules, the side chain flexibility of residues 21−30 in this lone helix C′ varies with a periodicity similar to that detected by EPR. In general, the parameter ΔH_0^{-1}, or M_s, obtained in spin-label EPR studies, is often called a measure of side chain mobility (*24*, *25*, *29*). However, it is also stated that M_s reflects changes in both order (S) and motion (τ_e) (*25*). Thus, helix C′ is a lone helix, with hydrophobic and hydrophilic faces. The side chains on the hydrophobic face are more ordered and less flexible, whereas the side chains on the hydrophilic side are less ordered and more flexible. These side chain properties cannot be detected by NMR methods used to determine structures, but are detected by spin-label EPR. Thus, the asymmetric nature of helix C′ is easily revealed by ΔH_0^{-1} values, with smaller ΔH_0^{-1} values for the residues on the hydrophobic face of the helix and larger ΔH_0^{-1} values for the residues on the hydrophilic face of the helix. These results are in good agreement with the heptad assignments, with residues 21, 24, and 28 assigned to "a" and "d" positions (*19*).

The addition of TFE promotes helical formation [increases the helicity of our peptides by 20−30% (*19*)], and as we mentioned before, TFE is a solvent known to affect hydrogen bonding and solvent structure and thus can affect the hydrophobic face of helix C′ (*37*, *38*). It is interesting to note that the variations in ΔH_0^{-1} values decreased in the presence of TFE to an extent that the periodicity pattern was much less prominent than that without TFE, suggesting that helix C′ is more symmetric in TFE solution.

The native gel data show that when the residue at position 24 or 28 was replaced with spin-labeled cysteine, the peptide would not associate with β peptide at micromolar concentrations. Thus, the simple ΔH_0^{-1} versus residue position plot from cysteine-scanning EPR data identified the hydrophobic and hydrophilic faces of this amphipathic helix C′, and revealed residues that are functionally important. The residues with small ΔH_0^{-1} values, such as residues 21, 25, 28, and 29, are on the hydrophobic face of the helix and therefore are likely to be critical in tetramerization. Mutations at some of these sites are known to be deleterious. Mutations I24S [Spectrin Lograno (*45*)] and R28X [Spectrin Corbeil, R28H, for example (*46*)] have been identified clinically (*47*). Residue R28 is known to be a "hot spot" in spectrin (*48*) and may be uniquely involved in the tetramerization process. Our NMR studies of R28S in SpαI-1−156 suggested that the mutated helix C′ may transiently, on the NMR time scale, associate with helix A_1 and helix C_1 (the AC face of the following structural domain) (*49*). The R28S substitution deletes the cationic surface side chain, and thus may permit the transient association, giving rise to exchange effects in the NMR spectrum.

EPR data suggest that mutations at residues 21, 25, and 29 may also lead to clinical symptoms.

Structure of the β-Spectrin Partial Domain. Structural information about the β spectrin partial domain is mostly derived from sequence predictions at this time, suggesting

two helical segments, similar to the first two helices (helix A and helix B) in a spectrin structural domain. Our CD studies suggest that the two helices are not associated (*19*).

The βC partial domain consists of more than 60 amino acid residues, making a peptide similar to SpαI-1−156, consisting of the partial domain plus one full structural domain, making it too large and difficult for high-resolution NMR studies. A smaller peptide, consisting of the sequence of only the β partial domain, was insoluble in buffers (L. W.-M. Fung, unpublished observation) and thus difficult to assess in structural studies. Crystal growth of intact spectrin has not been successful for X-ray diffraction studies. Thus, cysteine-scanning spin-label EPR studies appear to be ideal for secondary structural information of the partial domain at the C-terminal end of βI spectrin that are critical in tetramerization.

The $\Delta H_0^{-1}/M_s$ values of the region consisting of residues 2008−2018 exhibited a periodicity of 3.5−4, again suggesting a helical backbone for this region (for simplicity, we refer to this region as helix A′). The ΔH_0^{-1} values at positions 2008, 2011, 2014, and 2018 were relatively low, thus indicating that these were the residues on the hydrophobic side of helix A′. It is not clear at this time why the ΔH_0^{-1} values at position 2008 were particularly low. It is reassuring to know that residues at positions 2011, 2014, and 2018 are assigned to "a" and "d" heptad positions (*19*). Interestingly, native gel results showed that, when each of the residues at these positions was replaced with a spin-labeled cysteine residue, its ability to bind to its partner, the SpαI peptide, was abolished, suggesting that these residues were at the "binding side" of helix A′.

For the region consisting of residues 2060−2076, EPR data clearly showed that residues at positions 2060−2070 exhibited periodicity for the ΔH_0^{-1} values, with residues at positions 2061, 2065, and 2068 exhibiting low values. Thus, the region consisting of residues 2060−2070 was in a helical conformation, with residues at positions 2061, 2065, and 2068 on the hydrophobic side of the helix. Again for simplicity, we refer to this region as helix B′. Since we did not scan the region between positions 2019 and 2059, our results did not demonstrate whether there were two helices in this region. We only demonstrated that both regions (residues 2008−2018 and residues 2060−2070) were helical. When each of the three residues at positions 2061, 2065, and 2068 was replaced with a spin-labeled cysteine residue, its ability to associate with SpαI was abolished, suggesting that these residues were at the binding side of helix B′.

One of the interesting EPR results was that for the region scanning residues 2071−2076. This region clearly did not exhibit a periodicity in the ΔH_0^{-1} values, and the values were relatively large, indicating that these residues exhibited rather flexible motions, suggesting a disordered conformation in this region. Thus, this helical region ends around residue 2070 or 2071, in good agreement with our previous studies (*27*). We prepared recombinant βI peptides of different lengths, all starting at position 1898, but terminating at position 2070, 2071, 2072, or 2073, and showed that the peptide that terminates at position 2072 or 2073 associates with SpαI-1−156. However, peptides that terminate at a position prior to position 2072 do not associate with SpαI-1−156, suggesting that the C-terminal segment of βI spectrin, starting from residue 2073, is in a disordered conformation and is not critical to spectrin tetramer formation.

Our EPR data suggest that mutations of residues at the hydrophobic face of a helix or helices (at positions 2011, 2014, 2018, 2061, 2065, and 2068) will be deleterious. The known clinical mutations in the regions we studied are at positions 2018 (*50*), 2019 (*51*), 2061 (*52*), and 2069 (*53*).

In summary, this work provides strong experimental evidence that the region identified via sequence homology as the partial domain in the C-terminus of βI spectrin consists of helical regions, with the helix ending around residue 2070 and the region with residues 2071−2076 assuming a disordered conformation. Furthermore, our results revealed the amphipathic nature of the helical regions, with residues 2008, 2022, 2024, and 2018, and residues 2061, 2065, and 2068 at the hydrophobic side, and probably critical for αN−βC association at the tetramerization site.

ACKNOWLEDGMENT

We thank Dr. B. G. Forget of Yale University School of Medicine (New Haven, CT) for the cDNA of erythroid spectrin.

REFERENCES

1. Broderick, M. J., and Winder, S. J. (2005) Spectrin, α-Actinin, and Dystrophin, *Adv. Protein Chem. 70*, 203−46.
2. Djinovic-Carugo, K., Gautel, M., Ylanne, J., and Young, P. (2002) The spectrin repeat: A structural platform for cytoskeletal protein assemblies, *FEBS Lett. 513*, 119−23.
3. Bennett, V., and Baines, A. J. (2001) Spectrin and Ankyrin-Based Pathways: Metazoan inventions for integrating cells into tissues, *Physiol. Rev. 81*, 1353−92.
4. Giorgi, M., Cianci, C., Gallagher, P., and Morrow, J. S. (2001) Spectrin oligomerization is cooperatively coupled to membrane assembly: A linkage targeted by many hereditary hemolytic anemias? *Exp. Mol. Pathol. 70*, 215−30.
5. Kordeli, E. (2000) The spectrin-based skeleton at the postsynaptic membrane of the neuromuscular junction, *Microsc. Res. Tech. 49*, 101−7.
6. Gascard, P., and Mohandas, N. (2000) New insights into functions of erythroid proteins in nonerythroid cells, *Curr. Opin. Hematol. 7*, 123−9.
7. DeMatteis, M. A., and Morrow, J. S. (2000) Spectrin tethers & mesh in the biosynthetic pathway, *J. Cell Sci. 113*, 2331−43.
8. Goodman, S. R. (1999) Discovery of nonerythroid spectrin to the demonstration of its key role in synaptic transmission, *Brain Res. Bull. 50*, 345−6.
9. Beck, K. A., and Nelson, W. J. (1998) A spectrin membrane skeleton of the Golgi complex, *Biochim. Biophys. Acta 1404*, 153−60.
10. Yu, J., Fischman, D., and Steck, T. L. (1973) Selective solubilization of proteins & phospholipids from red blood cell by nonionic detergents, *J. Supramol. Struct. 1*, 233−48.
11. Speicher, D. W., and Marchesi, V. T. (1982) Spectrin domains: Proteolytic susceptibility as a probe of protein structure, *J. Cell. Biochem. 18*, 479−92.
12. Delaunay, J., and Dhermy, D. (1993) Mutations involving the spectrin heterodimer contact site: Clinical expression & alterations in specific function, *Semin. Hematol. 30*, 21−33.
13. Perrotta, S., Iolascon, A., De Angelis, F., Pagano, L., Colonna, G., Cutillo, S., and Miraglia del Giudice, E. (1995) Spectrin Anastasia ($\alpha^{I/78}$): A new spectrin variant (α45 Arg → Thr) with moderate elliptocytogenic potential, *Br. J. Haematol. 89*, 933−6.
14. Speicher, D. W., Knowles, W. J., and Marchesi, V. T. (1980) Identification of proteolytically resistant domains of human-erythroid spectrin, *Proc. Natl. Acad. Sci. U.S.A. 77*, 5673−7.
15. Speicher, D. W., DeSilva, T. M., Speicher, K. D., Ursitti, J. A., Hembach, P., and Weglarz, L. (1993) Location of the human red cell spectrin tetramer binding site & detection of a related "closed" hairpin loop dimer using proteolytic footprinting, *J. Biol. Chem. 268*, 4227−35.

16. Morrow, J., and Marchesi, V. T. (1981) Self-assembly of spectrin oligomers in vitro: A basis for a dynamic cytoskeleton, *J. Cell Biol. 88*, 463−8.
17. DeSilva, T. M., Peng, K. C., Speicher, K. D., and Speicher, D. W. (1992) Analysis of human red cell spectrin tetramer (head-to-head) assembly using complementary univalent peptides, *Biochemistry 31*, 10872−8.
18. Sumandea, C. A., and Fung, L. W.-M. (2005) Mutational Effects at the Tetramerization Site of Nonerythroid Alpha Spectrin, *Mol. Brain Res. 136*, 81−90.
19. Mehboob, S., Luo, B. H., and Fung, L. W.-M. (2001) $\alpha\beta$ spectrin association: A model system to mimic helical bundling at the tetramerization site, *Biochemistry 40*, 12457−64.
20. Speicher, D. W., and Marchesi, V. T. (1984) Erythrocyte spectrin is comprised of many homologous triple helical segments, *Nature 311*, 177−80.
21. Park, S., Caffrey, M., Johnson, M. E., and Fung, L. W.-M. (2003) Solution Structural Studies on Human Erythrocyte α Spectrin Tetramerization Site, *J. Biol. Chem. 278*, 21837−44.
22. Yan, Y. E., Winograd, E., Viel, A., Cronin, T., Harrison, S. C., and Branton, D. (1993) Crystal structure of the repetitive segments of spectrin, *Science 262*, 2027−30.
23. Grum, V. L., Li, D., MacDonald, R. I., and Mondragon, A. (1999) Structures of two repeats of spectrin suggest models of flexibility, *Cell 98*, 523−35.
24. Hubbell, W. L., Cafiso, D. S., and Altenbach, C. (2000) Identifying conformational changes with site-directed spin labeling, *Nat. Struct. Biol. 7*, 735−9.
25. Columbus, L., and Hubbell, W. L. (2002) A new spin on protein dynamics, *Trends Biochem. Sci. 27*, 288−95.
26. Luo, B. H., Mehboob, S., Hurtuk, M. G., Pipalia, N. H., and Fung, L. W.-M. (2002) Residues at and before position 2072 (Thr) of β-spectrin are important for helical bundling of α-β spectrin complex, *Eur. J. Haematol. 68*, 73−9.
27. Cherry, L., Menhart, N., and Fung, L. W.-M. (2000) Spin-Label EPR Structural Studies of the N-terminus of α-Spectrin, *FEBS Lett. 466*, 341−5.
28. Lusitani, D. M., Qtaishat, N., LaBrake, C. C., Yu, R. N., Davis, J., Kelley, M. R., and Fung, L. W.-M. (1994) The first human α-spectrin structural domain begin with serine, *J. Biol. Chem. 269*, 25955−8.
29. Mchaorab, H. S., Lietzow, M. A., Hideg, K., and Hubbell, W. L. (1996) Motion of spin-labeled side chains in T4 lysozyme. Correlation with protein structure and dynamics, *Biochemistry 35*, 7692−704.
30. Jorgensen, W. L., Chandrasekhar, J., Madura, J., and Klein, M. L. (1983) Comparison of Simple Potential Functions for Simulating Liquid Water, *J. Chem. Phys. 79*, 926−35.
31. Case, D. A., Pearlman, D. A., Caldwell, J. W., Cheatham, T. E., III, Wang, J., Ross, W. S., Simmerling, C. L., Darden, T. A., Merz, K. M., Stanton, R. V., Cheng, A. L., Vincent, J. J., Vincent, M., Crowley, V., Tsui, V., Gohlke, H., Radmer, R. J., Duan, Y., Pitera, J., Massova, I., Seibel, G. L., Singh, U. C., Weiner, P. K., and Kollman, P. A. (2002) *AMBER 7*, University of California, San Francisco.
32. Wang, J., Cieplak, P., and Kollman, P. A. (2000) How well does a restrained electrostatic potential (RESP) model perform in calculating conformational energies of organic and biological molecules? *J. Comput. Chem. 21*, 1049−74.
33. Darden, T., York, D., and Pedersen, L. (1993) Particle mesh Ewald-an Nlog(N) method for Ewald sums in large systems, *J. Chem. Phys. 98*, 10089−92.
34. Ryckaert, J. P., Ciccotti, G., and Berendsen, H. J. C. (1977) Numerical integration of the Cartesian equations of motion of a system with constraints: Molecular dynamics of *n*-alkanes, *J. Comput. Phys. 23*, 327−41.
35. Berendsen, H. J. C., Postma, J. P. M., van Gunsteren, M. F., DiNola, A., and Haak, J. R. (1984) Molecular dynamics with coupling to an external bath, *J. Chem. Phys. 81*, 3684−90.
36. Zhao, M., Zen, K. C., Hernandez-Borrell, J., Altenbach, C., Hubbell, W. L., and Kaback, H. R. (1999) Nitroxide scanning electron paramagnetic resonance of helices IV and V and the intervening loop in the lactose permease of *Escherichia coli*, *Biochemistry 38*, 15970−7.
37. Buck, M. (1998) Trifluoroethanol and colleagues: Cosolvents come of age. Recent studies with peptides and proteins, *Q. Rev. Biophys. 31*, 297−355.
38. Chitra, R., and Smith, P. E. (2001) Properties of 2,2,2-trifluoroethanol and water mixtures, *J. Chem. Phys. 114*, 426−35.
39. Gente, G., and La Mesa, C. (2000) Water-trifluorethanol mixtures: Some physicochemical properties, *J. Surf. Chem. 29*, 1159−72.
40. *Handbook of Chemistry & Physics* (2003) 84th ed., pp 8−83, CRC Press, Cleveland, OH.
41. Cohen, C., and Parry, D. A. D. (1986) α-helical coiled-coils: A widespread motif in proteins, *Trends Biochem. Sci. 11*, 245−8.
42. Fasman, G. D. (1989) *Prediction of Protein Structure and the Principles of Protein Conformation*, Plenum Press, New York.
43. Eisenberg, D., Weiss, R. M., and Terwilliger, T. C. (1984) The hydrophobic moment detects periodicity in protein hydrophobicity, *Proc. Natl. Acad. Sci. U.S.A. 81*, 140−4.
44. Perozo, E., Cortes, D. M., and Cuello, L. G. (1998) Three-dimensional architecture and gating mechanism of a K^+ channel studied by EPR spectroscopy, *Nat. Struct. Biol. 5*, 459−69.
45. Parquet, N., Devaux, I., Boulanger, L., Galand, C., Boivin, P., Lecomte, M. C., Dhermy, D., and Garbarz, M. (1994) Identification of three novel spectrin α I/74 mutations in hereditary elliptocytosis: Further support for a triple-stranded folding unit model of the spectrin heterodimer contact site, *Blood 84*, 303−8.
46. Garbarz, M., Lecomte, M. C., Feo, C., Devaux, I., Picat, C., Lefebvre, C., Galibert, F., Gautero, H., Bournier, O., and Galand, C. (1990) Hereditary pyropoikilocytosis and elliptocytosis in a white French family with the spectrin α I/74 variant related to a CGT to CAT codon change (Arg to His) at position 22 of the spectrin α I domain, *Blood 75*, 1691−8.
47. Gallagher, P., and Forget, B. G. (1996) Hematologically important mutations: Spectrin variants in hereditary elliptocytosis and hereditary pyropoikilocytosis, *Blood Cells, Mol., Dis. 22*, 254−8.
48. Coetzer, T. L., Sahr, K., Prchal, J., Blacklock, H., Peterson, L., Koler, R., Doyle, J., Manaster, J., and Palek, J. (1991) Four different mutations in codon 28 of α spectrin are associated with structurally and functionally abnormal spectrin α I/74 in hereditary elliptocytosis, *J. Clin. Invest. 88*, 743−9.
49. Park, S., Johnson, M. E., and Fung, L. W.-M. (2002) NMR Studies of Mutations at the Tetramerization Region of Human α Spectrin, *Blood 100*, 283−8.
50. Sahr, K. E., Coetzer, T. L., Moy, L. S., Derick, L. H., Chishti, A. H., Jarolim, P., Lorenzo, F., Miraglia del Giudice, E., Iolascon, A., and Gallanello, R. (1993) Spectrin Cagliari: An Ala → Gly substitution in helix 1 of β spectrin repeat 17 that severely disrupts the structure and self-association of the erythrocyte spectrin heterodimer, *J. Biol. Chem. 268*, 22656−62.
51. Gallagher, P. G., Weed, S. A., Tse, W. T., Benoit, L., Morrow, J. S., Marchesi, S. L., Mohandas, N., and Forget, B. G. (1995) Recurrent fatal hydrops fetalis associated with a nucleotide substitution in the erythrocyte β-spectrin gene, *J. Clin. Invest. 95*, 1174−82.
52. Glele-Kakai, C., Garbarz, M., Lecomte, M. C., Leborgne, S., Galand, C., Bournier, O., Devaux, I., Gautero, H., Zohoun, I., Gallagher, P. G., Forget, B. G., and Dhermy, D. (1996) Epidemiological studies of spectrin mutations related to hereditary elliptocytosis and spectrin polymorphisms in Benin, *Br. J. Haematol. 95*, 57−66.
53. Maillet, P., Inoue, T., Kanzaki, A., Yawata, A., Kato, K., Baklouti, F., Delaunay, J., and Yawata, Y. (1996) Stop codon in exon 30 (E2069X) of β-spectrin gene associated with hereditary elliptocytosis in spectrin Nagoya, *Hum. Mutat. 8*, 366−8.

BI051009M